NON-LINEAR STRUCTURAL DYNAMICS ASPECTS OF THE AERIAL REFUELLING BOOM SYSTEM

F. Arévalo, S. Claverías, and H. Climent
Structural Dynamics and Aeroelasticity Department
AIRBUS Defence & Space
Paseo John Lennon s/n, 28906 Getafe (Madrid), Spain
felix.arevalo@airbus.com, sebastian.claverias@airbus.com, and hector.climent@airbus.com

Keywords: A330-MRTT, Boom, Buffet, Dynamic Loads.

Abstract: AIRBUS Defence & Space (DS) has designed, manufactured, and successfully sold the advanced refuelling tanker- and receiver-role aircraft A330-MRTT. The A330-MRTT is based on the AIRBUS A330 platform that is modified for including the following refuelling devices: two under-wing pods, an Aerial Refuelling Boom System (ARBS), a slipway-type receptacle for receiving fuel and, as option, a Fuselage Refuelling Unit (FRU) installed at the aircraft belly.

The Boom system is a deployable mast installed at the A330-MRTT rear fuselage with the aim of dispatching fuel at high rate. Once deployed, the Boom is free to rotate (lateral *roll* and vertical *pitch* degrees of freedom) relative to the tanker. Control over pitch and roll is obtained through aerodynamic vanes (Ruddervators) located at its rearward tip. In addition, an internal probe can be fore and aft extended to contact the receiver aircraft.

The design of a Refuelling Boom System is a challenging process due to the inherent non-linearities associated to the rigid body large displacements. For example, the downward pitch-angle excursions lead to high angle of attack on the Ruddervators with non-clean unsteady aerodynamic loads that excite the structure (buffet). The characterization (flight tests), dynamic loads evaluation (computations), and design solutions to avoid long-term fatigue issues have been analyzed and are detailed into this paper.

On the other hand, the high-performance design concept of the AIRBUS DS leads to highly dynamic scenarios that exhibit a strong coupling between the rigid body and the flexible normal modes. This paper analyses a typical evasive scenario as example of complex simulation that combines structural nonlinearities, rigid body modes, and dynamic loads including flexible effects. The analytical simulation is based on the classical frequency-domain methods coupled with feedback-type forces to introduce the non-linear terms. The integral convolution theory is used to couple the linear and non-linear part of the system.

The paper shows that frequency-domain-based tools in combination with non-linear feedback loops are useful and robust tools to simulate complex non-linear dynamic load scenarios, showing fairly good results when comparing with flight test data.

1 INTRODUCTION

The design of a high-performance refuelling Boom requires considering aerodynamic and structural nonlinearities that result from the operation.

Detached-flow nonlinear aerodynamics induces mild buffeting at high speed/Mach when Boom rotates downward and reaches extreme pitch angles.

Structural nonlinearities arise from evasive-type manoeuvres with large rigid body excursions that lead the Boom to pass thru different operating modes which have different boundary conditions at the Boom-to-aircraft fitting (the roll/pitch joint).

Both buffet and evasive Safe Separation Assessment (SSA) manoeuvres have been characterized by flight tests on the A330-MRTT prototype #01 (Figure 1). This paper details the methods and procedures implemented in AIRBUS Defence & Space to deal with such nonlinearities. The engineering processes are all based on classical linear approaches supplemented with nonlinear features to cope with the particular nonlinearity. All results are compared with flight test data.

Figure 1 A330-MRTT tanker aircraft dispatching fuel thru the Boom to an F-16.

2 DESCRIPTION OF THE REFUELLING BOOM SYSTEM

2.1 A330-MRTT AIRCRAFT: ADVANCED REFUELLING TANKER

The A330-MRTT (Figure 2) is a military aircraft derived from the Airbus A330 civil aircraft which is equipped with refuelling devices to operate as tanker and receiver. The tanker-role refuelling devices consist on two under-wing pods, an Aerial Refuelling Boom System (ARBS) installed at the rear fuselage and, as option, a Fuselage Refuelling Unit (FRU) installed at the centre fuselage. The MRTT is able to receive fuel through the Universal Aerial Refuelling Receptacle Slipway Installation (UARSSI) located at the fuselage nose. Figure 2

([1]) details all these systems that are numbered from 1 to 4 according to the fuel rate capacity, being "1" the device with maximum fuel rate.

Figure 2: A330-MRTT aircraft with the refuelling devices (under-wing pods and ARBS) and the UARSSI receptacle at the fuselage nose ([1]).

2.2 AERIAL REFUELLING BOOM SYSTEM "ARBS"

The Boom system (Figure 3) is a flexible telescopic beam installed at the rear fuselage that is controlled by small wings-like called Ruddervators. The Boom is attached to the fuselage by means of an articulated joint (the "roll/pitch" joint, see Figure 4), which allows rigid body up/down motion (pitch rotation) and lateral motion (roll rotation).

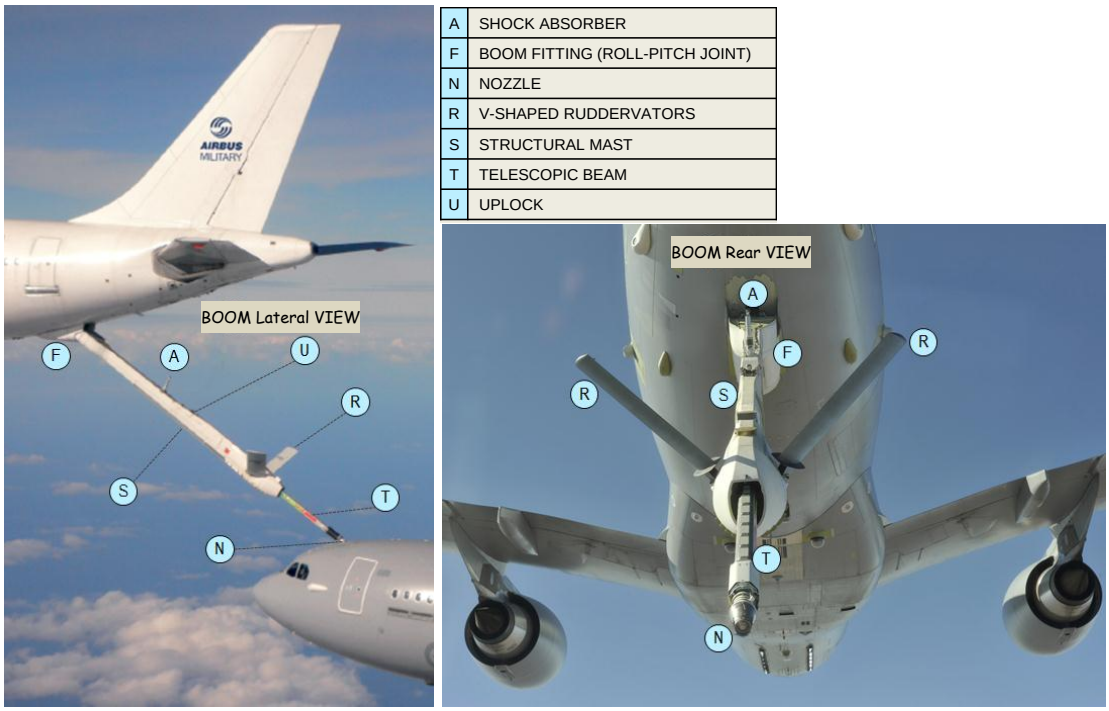

A	SHOCK ABSORBER
F	BOOM FITTING (ROLL-PITCH JOINT)
N	NOZZLE
R	V-SHAPED RUDDERVATORS
S	STRUCTURAL MAST
T	TELESCOPIC BEAM
U	UPLOCK

Figure 3: Boom system with its main structural components.

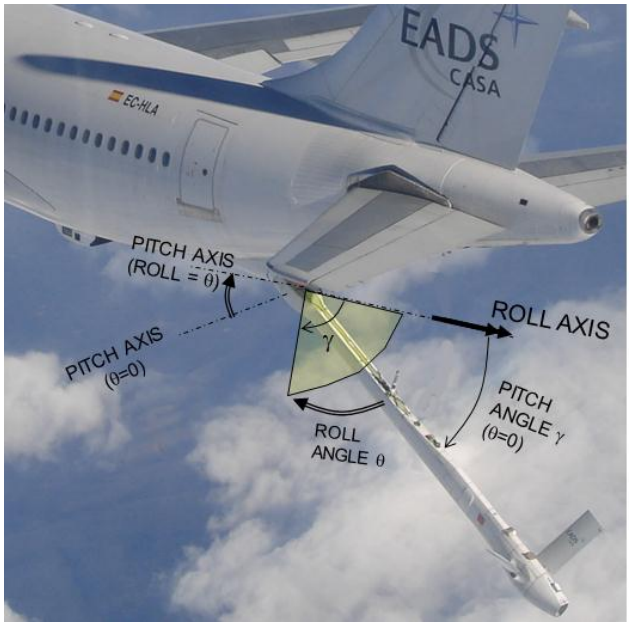

Figure 4 Free-flying Boom deployed configuration is controlled by the Ruddervators […]

When not operated, the Boom is maintained in the stowed position (Figure 2), restrained to the A330-MRTT thru the roll/pitch joint and three additional lateral and vertical fittings along the structural mast. The Boom is deployed by disengaging the lateral and vertical fittings what allows rotating down around the pivot point R_τ in the τ-mode (Figure 5), and varying τ angle from τ_{stowed} to $\tau_{deployed}$. Once $\tau_{deployed}$ is reached, the τ angle gets blocked and the γ-mode starts, which consists on free rotation around the pitch point R_γ of Figure 5. The pitch γ-angle is always geometrically restricted to $\gamma \geq \gamma_{min}$.

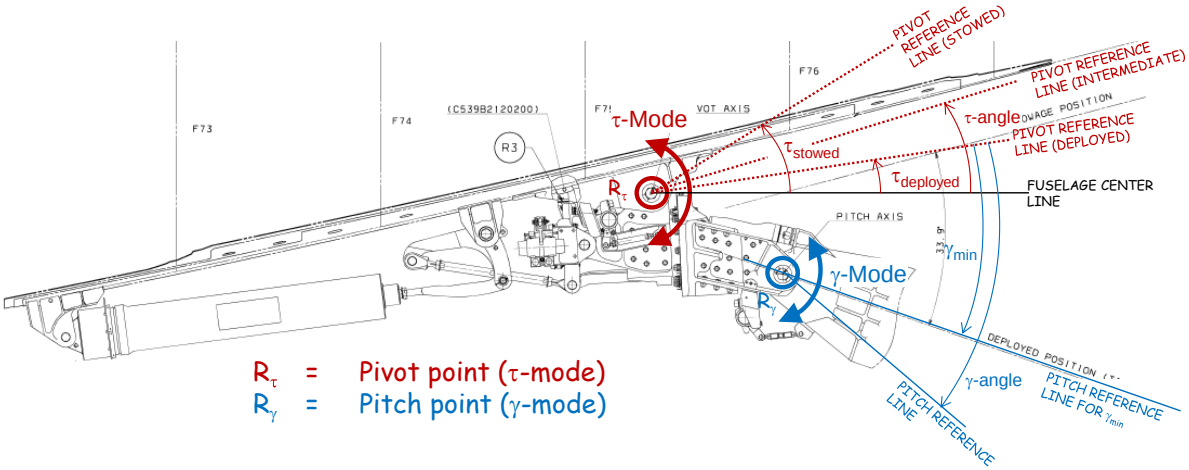

Figure 5 Roll/pitch joint with the two Boom operating modes in the deployed configuration: the τ-mode, with rotation around the pivot point R_γ and γ-mode, with rotation around the pitch point R_τ.

3 NON-LINEAR ASPECTS ON BOOM STRUCTURAL DYNAMICS

During a refuelling operation, the Boom resembles a morphing system with changes on the following properties ([2]):

1. Inertia: Boom fuel content varies in a range between zero and full of fuel.
2. Geometry: large excursions in pitch and roll and different positions of the telescopic beam change both structural and aerodynamic models orientation, which induces changes on flexible modes (Figure 6), unsteady aerodynamic influence coefficients, etc.
3. Boundary conditions (BCs): stowed, deployed free-flight, and deployed connected-to-receiver Boom configurations have different restrictions on the structural mast Boom-to-A/C fittings (stowed/deployed) and the telescopic beam nozzle (connected/unconnected).
4. Flight control laws: Ruddervators rotation is commanded by a flight-by-wire system whose design parameters depend on the flight condition and Boom attitude.

Previous changing properties introduce variations on the structural dynamics (normal modes) and aeroelastic (unsteady aerodynamics) models that can be tackled with a classical linearization procedure. However, there exist specific Boom operations where the linear approach is not accurate enough and nonlinearities are to be included into the aeroelastic simulations, e.g.:

1. Aerodynamic nonlinearities: mild buffet onset ([3]), high angle-of-attach flow detachment, etc.
2. Boom manoeuvring that involves local stiffness changes during the event: Boom pitch motion with transition from γ- to τ-mode and viceversa.
3. Impact loads: Boom nozzle impact loads, etc.

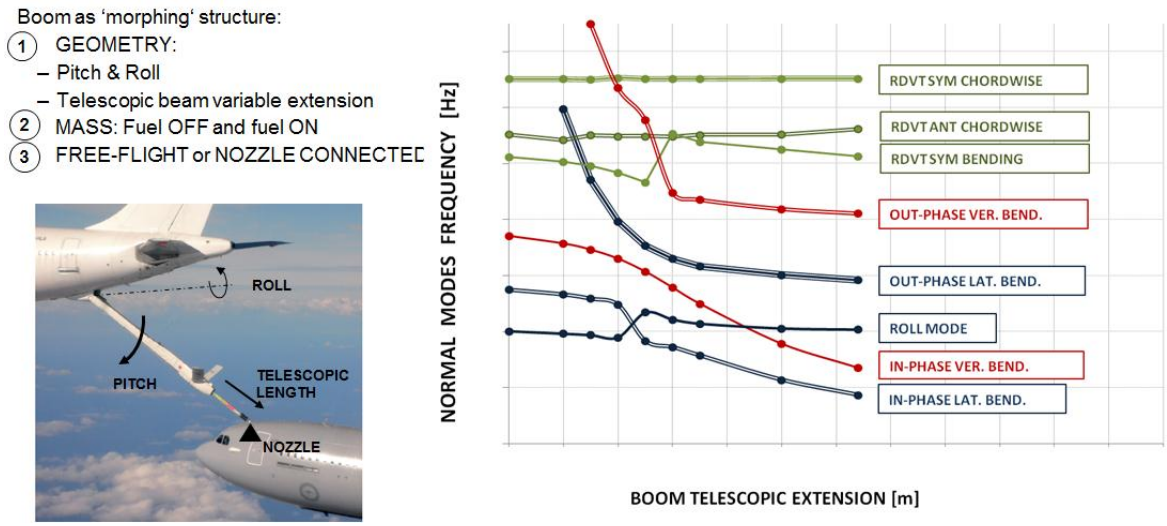

Figure 6 Boom normal modes frequencies as function of the telescopic beam extension.

Impact loads are best calculated with ad hoc explicit-type codes (PAMCRASH, DYTRAN, etc.). Buffet and local stiffness changes can be analysed with classical dynamic system solvers tuned to cope with the non-linear part of the problem. Next two sections will detail these two events, describing the phenomenon, the flight tests and aeroelastic simulations that supported the A330-MRTT certification process.

4 AERODYNAMIC NON-LINEARITIES: BUFFET

4.1 BOOM BUFFET ONSET CHARACTERIZATION

Figure 7 shows the Boom geometrical roll/pitch envelopes. Envelope A is the control envelope for free-flight (nozzle disconnected), while envelope C corresponds to the connected-to-receiver envelope. The nominal refuelling operation is performed around the centre of the connected-to-receiver envelope C (see label NOMINAL REFUELLING in Figure 7)

Figure 7 Boom geometrical roll/pitch envelopes: A=Boom control envelope and C=Boom connected envelope. Lower corner of envelope A corresponds to maximum pitch and, at high Mach number conditions, is the zone affected by mild buffet.

Figure 8 Lateral (Ny) and vertical (Nz) accelerometers to measure buffeting.

An extensive flight test campaign was performed with the Boom prototype (A330-MRTT MSN 747) for characterizing the Boom mast and ruddervators buffeting. At each flight condition KCAS/altitude, the Boom was positioned with the maximum pitch angle and roll varying between the minimum and maximum values, tracking the line 1-to-5 of Figure 7. Buffeting severity was estimated by measuring the Boom mast lateral and vertical accelerations at the location shown in Figure 8. The telescopic beam was positioned from retracted to full-extended in all flight conditions.

Flight tests showed that Boom is free from buffet when operating in the nominal roll/pitch envelope, although a mild buffet (with aerodynamic excitation equivalent to light turbulence) appears when operating at maximum pitch (corner point 2 in) and high speed/Mach number,

well outside the nominal refuelling conditions. Buffet non-linear aerodynamic excitation was associated to Boom mast and ruddervators flow detachment induced by the combination of local high angle of attack and high Mach number.

Buffet loads associated to this flight condition (highest speed/Mach and maximum pitch angle) were calculated and shown to be below the fatigue threshold for most of the Boom components. However, the comfort in the operation could be improved if vibrations associated to the buffeting were reduced. This last requirement led AIRBUS DS to search design solutions to minimize the buffeting.

4.2 DESIGN SOLUTIONS TO REDUCE BUFFETING

4.2.1 SOLUTION STRATEGIES

Two solution strategies were followed to minimize the Boom structural vibrations associated to the mild buffet:

1. Strategy #1 - Redefinition of the Boom control envelope: as buffet onset was restricted to speed/Mach flight conditions and pitch/roll attitude well outside of the nominal operation, the control envelope could be slightly reduced without penalty on the Boom performance. Subsequent flight tests on the reduced envelope showed relevant reduction on the structural vibrations without degrading the Boom performance.
2. Strategy #2 - Redesign of the Boom flight control laws: although strategy #1 above suppressed most of the structural vibrations, a low-frequency oscillation of the Boom was not mitigated as expected. When high Mach and maximum pitch buffeting occurred with the telescopic fully extended, an excitation of the low-frequency normal modes coupled with the Boom flight control laws and led to low-frequency non-damped limit cycle oscillations (LCO). This LCO behaviour was solved as explained in next section by adjusting specific design parameters of the Boom flight control laws.

4.2.2 ROOT CAUSE OF THE LOW-FREQUENCY LCOs

Boom motion is driven by the ruddervators deflections that are commanded by the operator (Boomer) thru a control system based on the fly-by-wire technology. Boom sensors distributed along the structure send back information of the Boom attitude (rigid body modes) that is used in a closed-loop feedback control. Notch filters are applied on the sensors signals to attenuate the flexible modes disturbances and obtain the rigid body contribution without altering the signal at the rest of the frequency spectrum. Practice shows that the notch filters introduce phase lags on the original signal that affect to a frequency band around each frequency that is notched. In this sense, notch filters are usually discarded in highly flexible structures with modal frequencies below a threshold in a way that notch filter applied on the lowest-frequency normal modes would induce phase lags on the rigid-body flight dynamics control.

The Boom system does exhibit this coupling phenomenon for the full-extended telescopic beam, the configuration with the lowest normal modes frequencies, and to attenuate the lateral flexible bending on the sensors signals the standard notch filtering was substituted by a procedure that allows removing the flexibility based on comparison between two sensors installed at the structural mast (Figure 9). The local rotation measured on each of the two sensors includes information of the rigid body modes (flight dynamics) plus the flexible

modes. The rigid body motion θ_{RB} is obtained by integrating the roll rate $d\theta_{RB}/dt$ that is in turn calculated as a combination of the two sensors signals by means of:

$$\frac{d\theta_{RB}}{dt} = f\left(\frac{d\theta_0}{dt}, \frac{d\theta_G}{dt}, k_{MF}\right) \quad (1)$$

where k_{MF} is a gain factor called *mixing factor*.

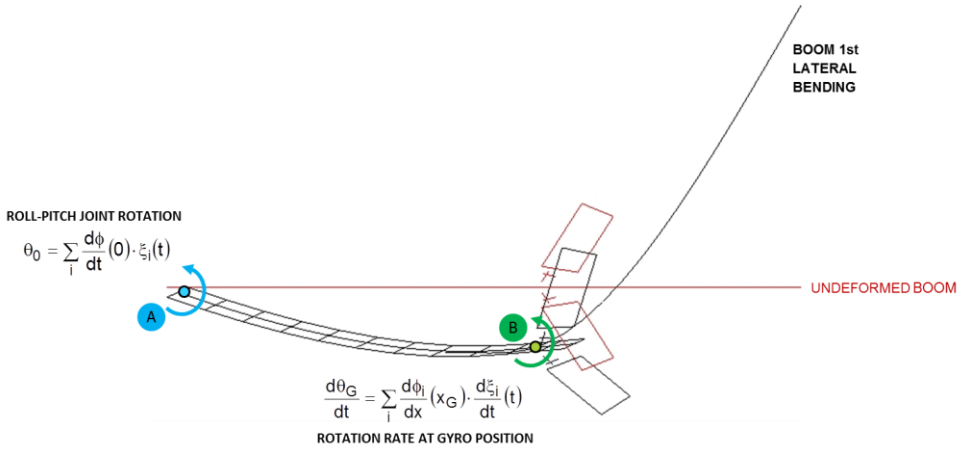

Figure 9 Sensors installed at the Boom structural mast to measure the Boom roll.

Preliminary values of the mixing factor were successfully tested without any coupling phenomenon. However, flights with buffeting conditions on full-extended configuration revealed low-frequency LCO oscillations associated to a lower-than-expected attenuation of the flexible normal modes. For these specific flight points and Boom configuration, the AIRBUS DS Flight Dynamics department readjusted the factor k_{MF}, solving the LCO-type Boom behaviour as shown in next section.

4.2.3 BUFFETING BEFORE AND AFTER INCLUDING THE TWO SOLUTION STRATEGIES

Figure 10 shows the root mean square of the lateral (N_y) and vertical (N_z) buffet-onset accelerations measured at the structural mast tip for three different telescopic beam extensions: full extended (black point), mid-extended (red points) and mid-to-retracted configuration. All these results do not include any of the two strategies described in section 4.2.1 for attenuating the mild buffet vibration levels. It is seen that LCO oscillations associated to the low attenuation of the lowest-frequency normal modes increase the lateral vibration levels (see label LCO OSCILLATIONS in Figure 10).

Figure 11 shows the lateral (N_y) and vertical (N_z) buffet-onset accelerations after introducing the two strategies for reducing the buffeting. All vibration levels dropped down dramatically after including the two redesign solution strategies, having the buffeting no impact on the Boom controllability as declared by the operator (Boomer).

Next step was to characterize the buffet loads associated to the improved-design remaining buffeting.

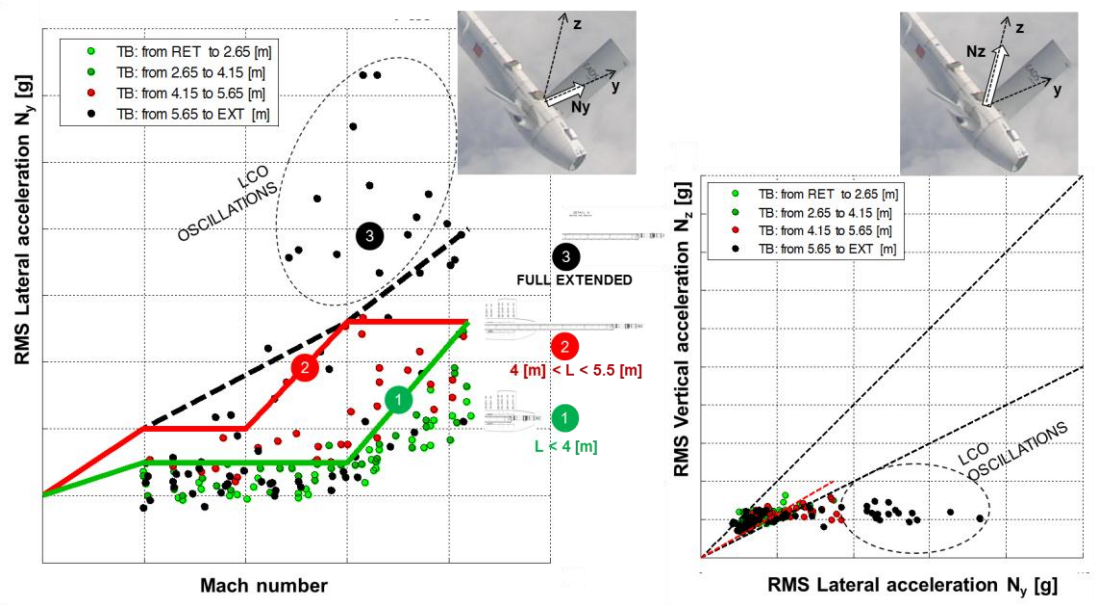

Figure 10 Root mean square (RMS) of the lateral (Ny) and vertical (Nz) accelerations measured at the Boom structural mast tip. These results were acquired BEFORE including the two solution strategies detailed in section 4.2.1.

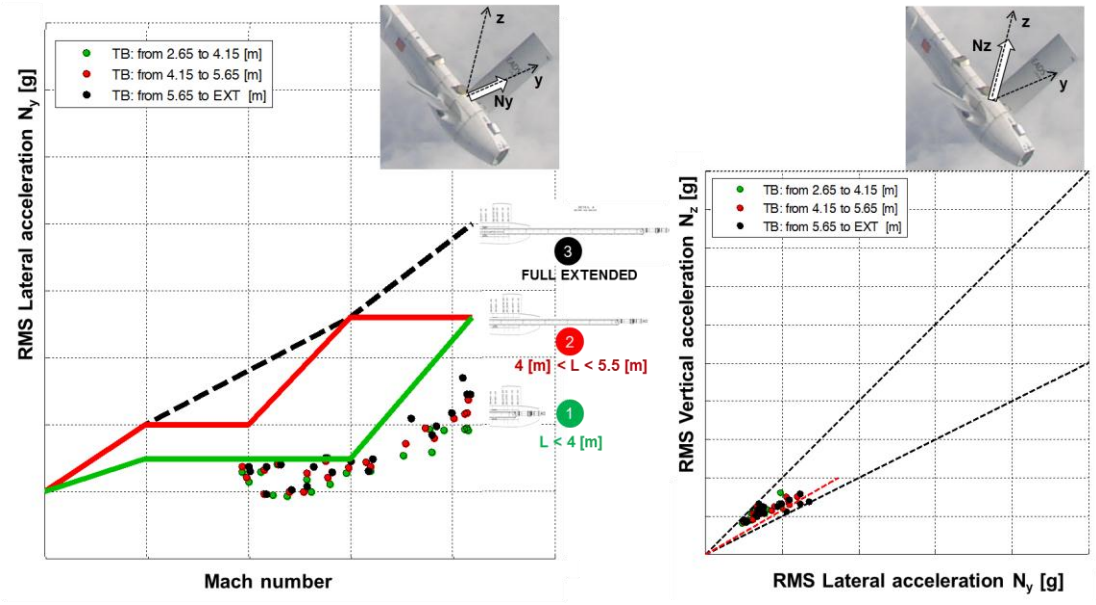

Figure 11 Root mean square (RMS) of the lateral (Ny) and vertical (Nz) accelerations measured at the Boom structural mast tip. These results were acquired AFTER including the two solution strategies detailed in section 4.2.1: reduce control envelope and modification of the Boom FCLs mixing factor.

4.3 MILD BUFFET LOADS CALCULATION PROCEDURE

Buffet is a random-type aerodynamic excitation that resembles the unsteady pressure loads generated in continuous turbulence (CT) encountering. As for CT random analyses, the power spectral density PSD_j of any structure magnitude (acceleration, load, stress,…) is related to the PSD_{IN} of the equivalent-to-buffet gust intensity by ([5])

$$PSD_j(\omega) = \left|FRF_j(\omega)\right|^2 \cdot PSD_{IN}(\omega) \cdot U_\sigma \qquad (4.3.1)$$

where FRF_j is the frequency response function of the magnitude *j*, which is calculated with the aeroelastic model matched to the Ground Vibration Test (GVT) and Flight Vibration Tests (FVT). The aeroelastic model includes the classical Doublet-Lattice method ([6]) for modelling the unsteady aerodynamics and FE model for the structure.

The equivalent-to-buffet CT power spectral density $PSD_{IN}{\cdot}U_\sigma$ is unknown, although it can be inferred from the in-flight measured lateral acceleration as sketched in Figure 12. The $PSD_{IN}{\cdot}U_\sigma$ values and shape of right column (blue line) of Figure 12 is the appropriate to induce the PSD of the lateral accelerometer of left column (red line).

Once $PSD_{IN}{\cdot}U_\sigma$ is known, the rest of magnitudes are calculated with [4.3.1].

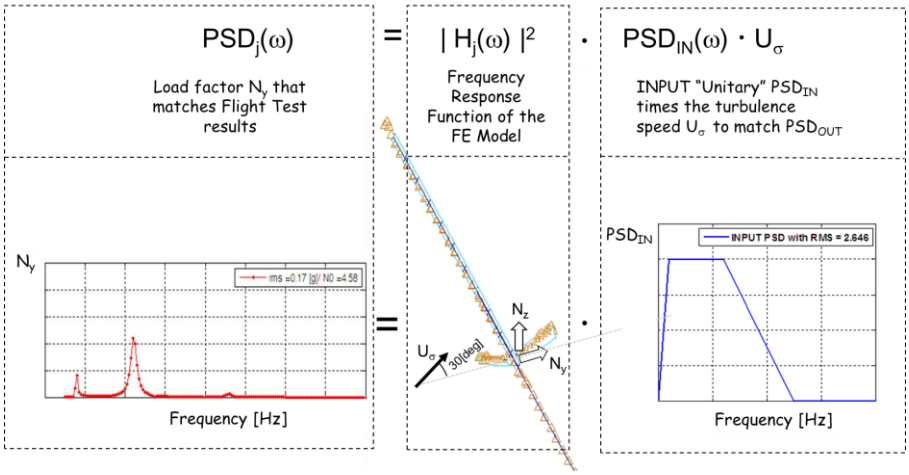

Figure 12 The PSD_{IN} of the equivalent-to-buffet CT intensity is obtained by matching PSD of the accelerometer Ny.

Calculations showed that buffeting levels were equivalent to structural vibrations caused by light turbulence, and induced buffet loads well below the fatigue threshold for most of the Boom components.

Therefore, the design solution was also considered as acceptable from loads standpoint.

5 STRUCTURAL NON-LINEARITIES: SAFE SEPARATION MANEUVER

5.1 INTRODUCTION

The Safe Separation Assessment (SSA) procedure is an evasive pitch-up manoeuvre that is performed to get a fast separation from the receiver aircraft in the event of any abnormal

situation during the refuelling operation. Boom is forced to rotate up (pitch) at high angular speed, passing thru the operating modes sketched in Figure 13, i.e.:

1. A-to-B: free rotation in γ-mode around the pitch point R_γ. The pitch reference line varies from A (initial deployed condition) to B (where γ reaches γ_{min}). There is no local rotation in τ-mode and therefore $\tau = \tau_{deployed}$ during all this phase.
2. Point B: the γ-angle is frozen at γ_{min} what forces the Boom to start the rotation in τ-mode around the pivot point R_τ.
3. C-to-D: rotation in τ-mode around the pivot point R_τ. There is no local rotation in γ-mode as $\gamma = \gamma_{min}$ during all this phase. The pivot reference line moves from C ($\tau = \tau_{deployed}$) to D, the maximum τ angle that depends on the pitch-up rate demanded by the Boomer. In all cases, the maximum limit angle τ_{stowed} is never reached.

Pitch-up SSA Maneuver

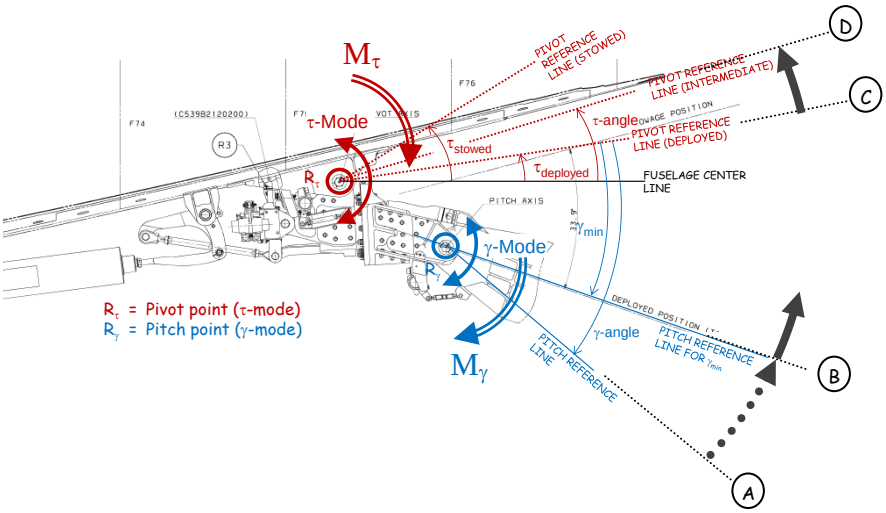

Figure 13 Left: A330-MRTT Boom connected to an F-16 aircraft. Dashed-line arc shows the γ-mode while full-line arc corresponds to the τ-mode phases that occur during the SSA manoeuvre. Right: roll/pitch joint functioning during the γ- and τ-mode phases.

As the SSA manoeuvre evolves, the roll/pitch joint behaves as a non-linear mechanism that introduces local moments Mγ and Mτ as shown in Figure 13 and detailed in Table 1. Next section will show how these nonlinearities have been considered in the simulations.

Finally, remark that the SSA manoeuvre can be performed starting from any roll angle. An initial roll angle different from zero will involve antisymmetric ruddervators deflection as the Boom tries to reach zero roll as the Boom approaches the fuselage of the tanker aircraft.

MODE	γ- or τ-angle	Local moment
γ-mode	$\gamma \geq \gamma_{min}$	$M_\gamma = 0$ (free rotation)
	$\gamma \leq \gamma_{min}$	$M_\gamma \rightarrow \infty$ (γ-angle is frozen at γ_{min})
τ-mode	$\tau \leq \tau_{deployed}$	$M_\tau \rightarrow \infty$ (τ-angle is frozen at $\tau_{deployed}$)
	$\tau_{deployed} \leq \tau \leq \tau_{stowed}$	$M_\tau = f(\tau)$ (non-linear function supplied by the pivot dampers manufacturer)
	$\tau \geq \tau_{stowed}$	$M_\tau \rightarrow \infty$ (τ-angle maximum is $\tau_{deployed}$)

Table 1 Local non-linear pitch (M_γ) and pivot (M_τ) moments at the roll/pitch joint as γ and τ angles evolve during the SSA maneuver.

5.2 SIMULATION PROCEDURE

The Boom dynamic loads model for simulating the SSA maneuver was based on the baseline linear aeroelastic model modified with the feedback forces of the nonlinear roll/pitch joint mechanism. As shown in Figure 14, the inertia, stiffness, and unsteady aerodynamic generalized matrices are calculated with MSC.NASTRAN, the integration of the aeroelastic equations including the nonlinear part is done with the Fortran-coded software called DYNRESP [7], and the integrated loads and interesting quantities of the model are obtained with the in-house Fortran-coded software DYNLOAD.

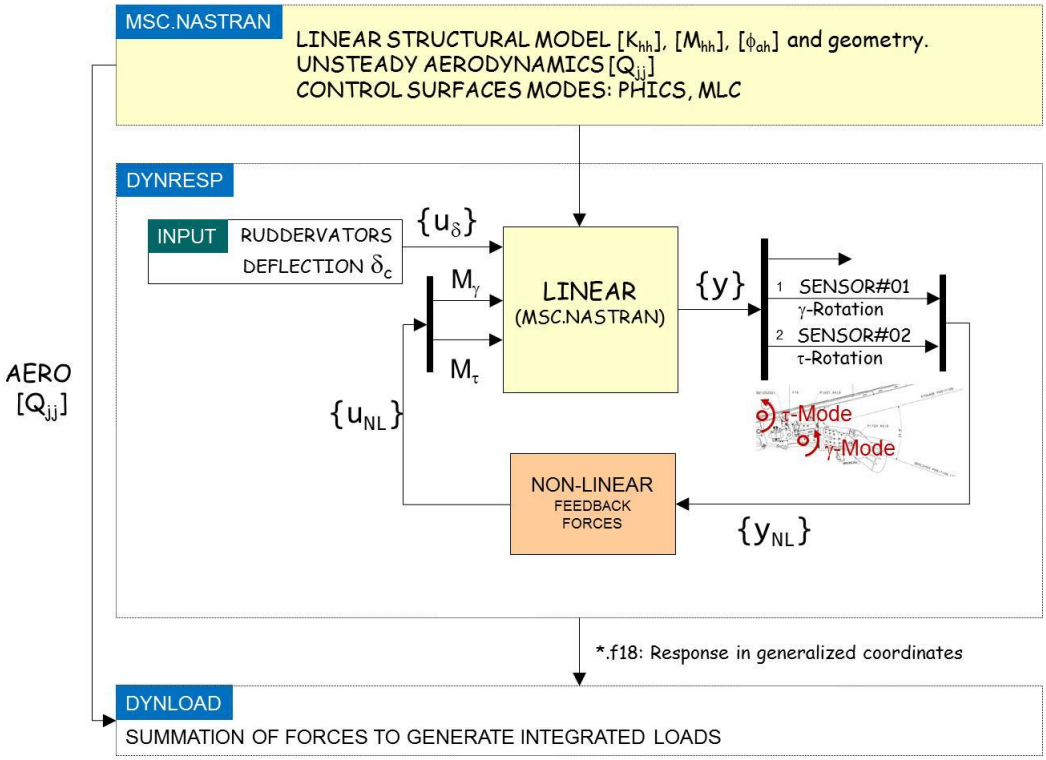

Figure 14 Linear and nonlinear blocks of the SSA maneuver simulations.

The calculation of the aeroservoelastic response to deterministic excitations with nonlinear control elements is based on a three-stage process that combines the frequency-domain linear aeroservoelastic response, the impulse response to control inputs, and time-domain simulations of the nonlinear elements ([7]):

1. Disconnection of the nonlinear block and calculation of two linear system transfer functions:
    a. $[H_\delta(i\omega)]$: Transfer function associated to the ruddervators deflection, i.e., $\{y(i\omega)\} = [H_\delta(i\omega)]\{u_\delta(i\omega)\}$
    b. $[H_u(i\omega)]$: Transfer function associated to the inputs to the linear block, i.e., $\{y_{NL}(i\omega)\} = [H_{NL}(i\omega)]\{u_{NL}(i\omega)\}$

2. Calculation of two time-domain responses of the linear system:
   a. $\{y_L(t)\}$: response to the commanded ruddervator deflection $\{\delta_c(t)\}$, calculated as inverse Fourier transform of $[H_\delta(i\omega)]\{\delta_c(i\omega)\}$, where $\{\delta_c(i\omega)\}$ is the Fourier transform of the commanded ruddervator rotation $\{\delta_c(t)\}$.
   b. $\{y_{LU}(t)\}$: response to unitary impulses at the inputs $\{u_{NL}\}$ of the linear block, calculated as inverse Fourier of $[H_{NL}(i\omega)]\{1\}$, where $\{1\}$ represents the Fourier transform of the unit impulses.
3. Calculation of the total nonlinear response by modifying the linear response $\{y_L(t)\}$ with a convolution integral that includes the nonlinear effect:

$$\{y(t)\} = \{y_L(t)\} + \int_0^t [y_{LU}(t-\tau)]\{u_{NL}(\tau)\}d\tau = \{y_L(t)\} + \int_0^t [y_{LU}(t-\tau)][F_{NL}(t, y, \dot{y}, \ddot{y}, \ldots)]\{y(\tau)\}d\tau$$

Where $\{u_{NL}(\tau)\}$ has been replaced by the functions of the nonlinear elements, i.e., $\{u_{NL}(t)\} = [F_{NL}(t, y, \dot{y}, \ddot{y}, \ldots)]\{y(t)\}$.

Previous convolution is numerically integrated to obtain the system nonlinear response $\{y(t)\}$.

5.3 SIMULATION RESULTS: COMPARISON WITH FLIGHT TESTS

Figure 15 shows the monitor stations, accelerations, and rotational degrees of freedom selected for characterizing the Boom response. First step of the simulations was to compare with flight test data to assess the reliability of the aeroelastic model.

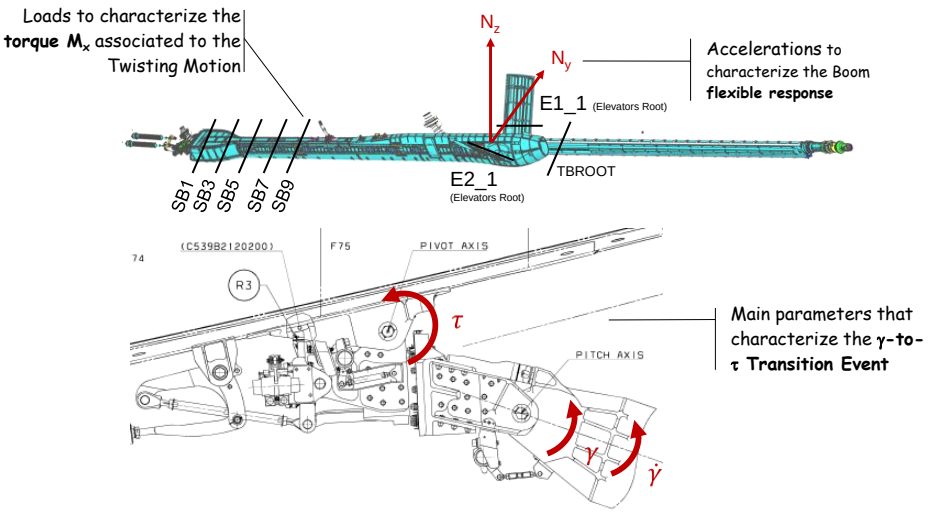

Figure 15 Boom monitor stations, accelerations, and rotation degrees of freedom that were selected are representative for characterizing the Boom response.

Test data was obtained from the extensive flight test campaign on the A330-MRTT prototype #01. The SSA manoeuvre was executed for different severity levels (pitch rate values) and initial roll angles. Figure 16 shows the comparison between flight test data and the aeroelastic model on the rotational degrees of freedom τ- and γ-angle and the vertical acceleration at the structural mast tip. The γ-angle decreases up to γ_{min}, instant in which the rotation around the pivot point (τ-angle) starts. The τ- and γ-angle time evolution show that the Boom rotational motion is well captured by the aeroelastic model, although the τ-angle evolution reveal that the model response is less damped than the flight test results. Peak values and shape of the vertical acceleration N_z is fairly well captured.

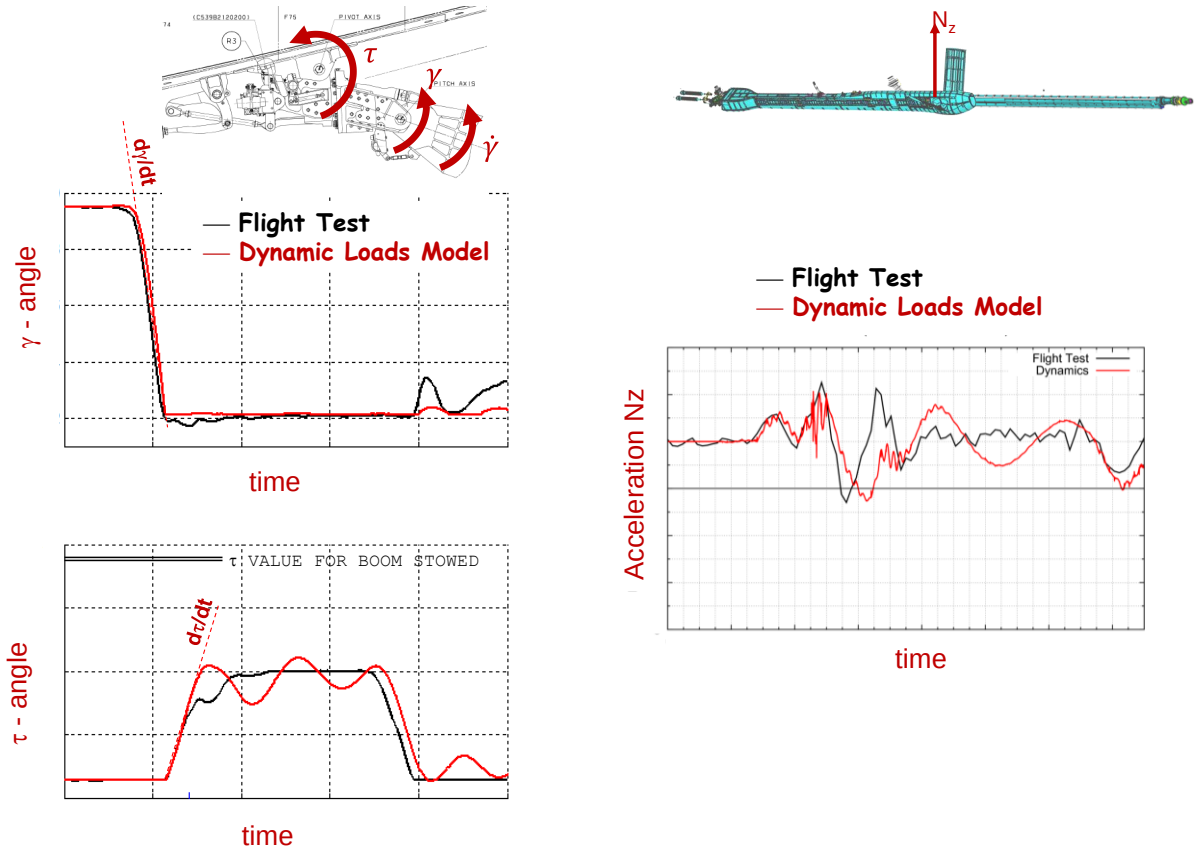

Figure 16 SSA maneuver results: comparison between flight test (black lines) and the aeroelastic model (red lines).

The torque moment calculated at the monitor station SB01 (structural mast root) is represented in Figure 17. The total torque (red line), which includes the initial 1g static loads plus the total (inertial plus aerodynamic) incremental loads, is shown to match the torque peak value estimated from the flight test evidences. In addition, the inertia contribution to the incremental loads (brown line) is shown to be coupled with the aerodynamic incremental loads (blue line), increasing the torque moment around 20% at the instant when the maximum torque is reached.

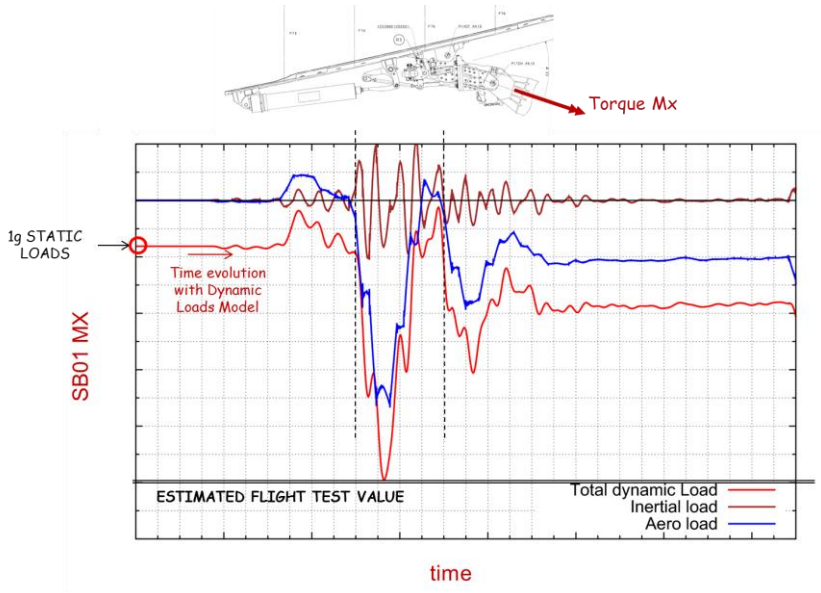

Figure 17 Torque moment time-history at station SB01 (structural mast root) calculated with the dynamic loads model. Red line corresponds to the total torque (incremental plus 1-g loads), blue line corresponds to the incremental torque associated to the unsteady aerodynamics, and brown line represents the incremental torque associated to the Boom inertia.

Once validated the loads model with flight test data, the SSA maneuver was simulated in the worst conditions (high dynamic pressure, maximum pitch rate, etc.) to obtain limit loads that were part of the Boom design loads.

6 CONCLUSIONS

This paper has analysed two events of the A330-MRTT Boom system in which the classical frequency-domain methods must be supplemented with nonlinear elements and/or supported by flight tests. The first one is the buffet onset, where nonlinear aerodynamic must be characterized by flight test data. The second one is the calculation of dynamic loads in manoeuvres with changing boundary conditions.

Buffeting is associated to high angle of attack of the Boom ruddervators (high pitch angle) combined with high Mach number, extreme conditions that are outside of the nominal control envelope. The buffeting levels were characterized by flight tests and two engineering solutions improved the Boom design: redefinition of the Boom control envelope and update of the mixing factor parameter of the flight control laws. The characterization of the buffeting and subsequent buffet loads calculations were performed by using classical random analysis validated with flight test data. Results included in this paper show that the two proposed solutions effectively reduced the buffeting levels to minimum values.

The paper has also analysed the pitch-up evasive manoeuvre SSA (Safe Separation Assessment) which has inherent structural nonlinearities associated to the transition between Boom operating modes. The nonlinear response has been simulated by completing the linear system solution with nonlinear terms calculated by using the time-domain convolution theory. This method was compared with flight test data obtaining reliable results.

7 REFERENCES

[1] Arévalo, F., "Aerial refuelling Boom system buffet onset at high speed and high angle: tests, simulations, and design solutions", *AIRBUS Workshop on Structural Dynamics and Aeroelasticity*, June-2014.

[2] Arévalo, F., Strömberg, A.M., Rosich, F., Anguita, L., and Climent, H., "Refueling Boom Aeroelasticity", *IFASD 2007*, Stockholm, June 2007.

[3] ESDU 87012, "An introduction to aircraft buffet and buffeting", 1987.

[4] Thorby, D., "Structural Dynamics and Vibration in Practice", Butterworth-Heinemann, 2008.

[5] Albano, E., and Rodden, W.P., "A Doublet Lattice Method for Calculating Lift Distributions on Oscillating Surfaces in Subsonic Flows", *AIAA Journal*, Vol. 7, No. 2, Feb. 1969, pp. 279-285, and Vol. 7, No. 11, Nov. 1969, p. 2192.

[6] Karpel M., "DYNRESP-8: Dynamic response of aircraft structures to gusts, maneuver commands, and direct forces – Theoretical manual", *KDC Report 2012-2*, 2012.

8 COPYRIGHT STATEMENT